

Supporting Information

F- or V-Induced Activation of (Co, Ni)₂P During Electrocatalysis for Efficient Hydrogen Evolution Reaction

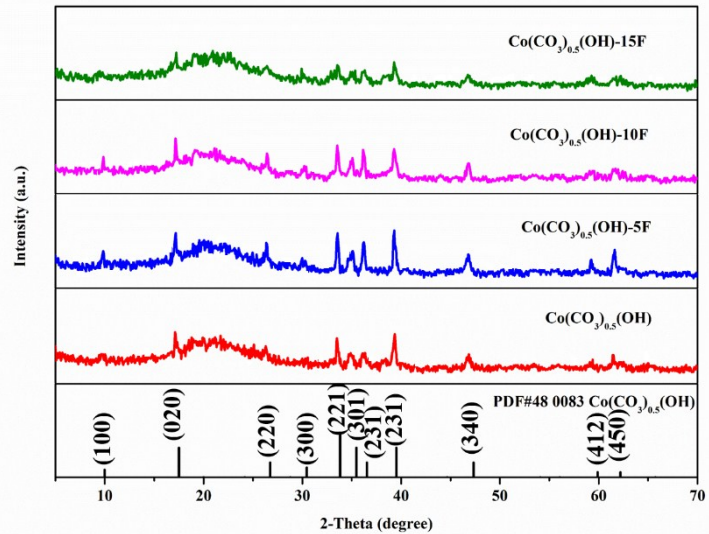
Li Liu, Keyu Tao, Huamei Dan, Yang Hai and Yun Gong*

Department of Applied Chemistry, College of Chemistry and Chemical Engineering, Chongqing University, Chongqing 401331, P. R. China. E-mail: gongyun7211@cqu.edu.cn; Tel: +86-023-65678932

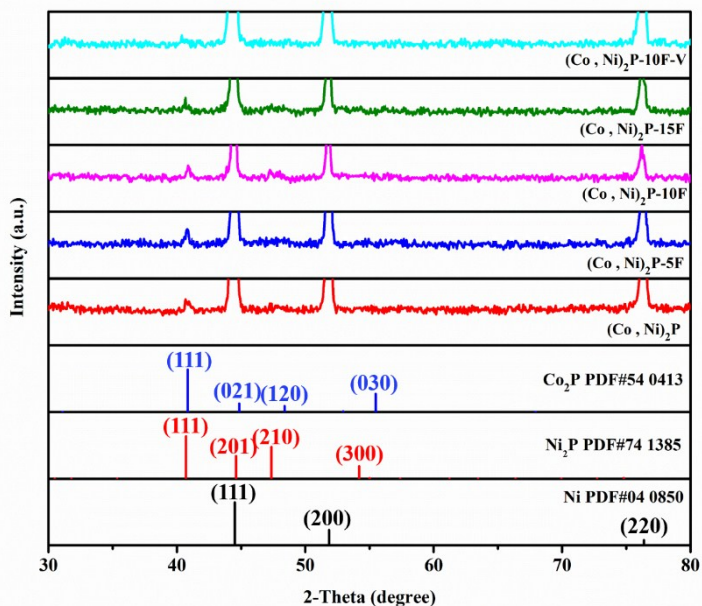
Table S1 The names of the samples synthesized under different conditions.

	Co(NO ₃) ₂ · 6H ₂ O (mg)	Urea (mg)	NH ₄ F (mg)	Na ₃ VO ₄ in the second step (mg)	After phosphorization	After 10h-electrolysis at -0.1 V vs Hg/HgO
Co(CO ₃) _{0.5} (OH)	32	33.6	0	/	(Co, Ni) ₂ P	Post-(Co, Ni) ₂ P
Co(CO ₃) _{0.5} (OH)-5F	32	33.6	5	/	(Co, Ni) ₂ P-5F	Post-(Co, Ni) ₂ P-5F
Co(CO ₃) _{0.5} (OH)-10F	32	33.6	10	/	(Co, Ni) ₂ P-10F	Post-(Co, Ni) ₂ P-10F
Co(CO ₃) _{0.5} (OH)-15F	32	33.6	15	/	(Co, Ni) ₂ P-15F	Post-(Co, Ni) ₂ P-15F
Co(CO ₃) _{0.5} (OH)-10F-V	32	33.6	10	6.9	(Co, Ni) ₂ P-10F -V	Post-(Co, Ni) ₂ P-10F -V

(a)



(b)



(c)

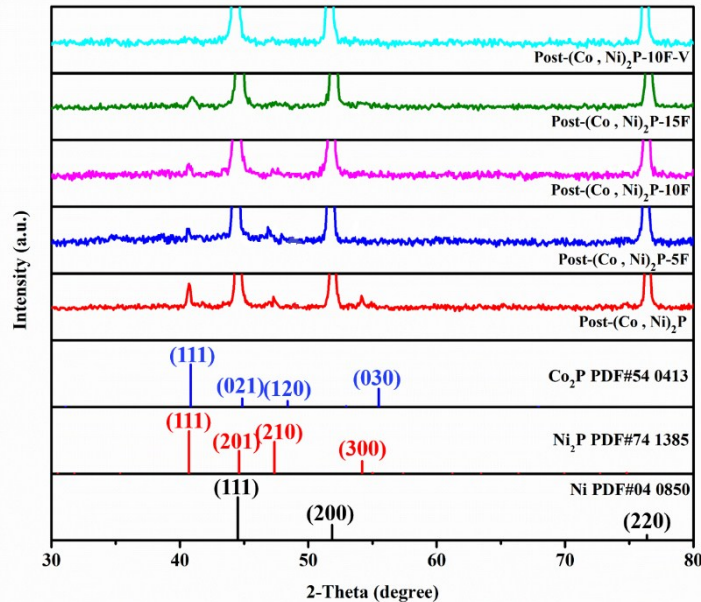
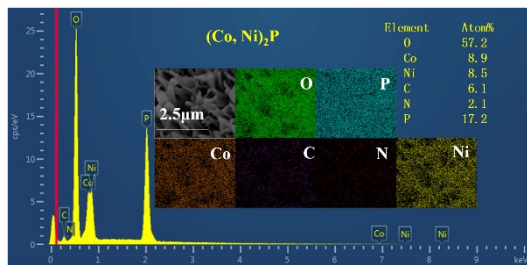
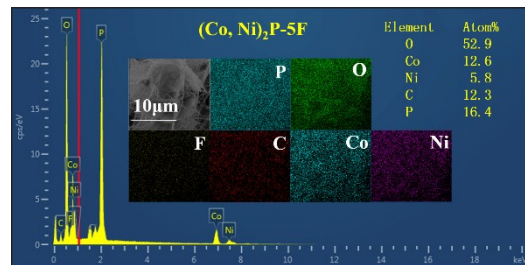


Figure S1 XRD patterns of $\text{Co}(\text{CO}_3)_{0.5}(\text{OH})/\text{NF}$ precursors (a), metal phosphides/NF (b), Post-metal phosphides/NF (c) and the standard profiles of $\text{Co}(\text{CO}_3)_{0.5}(\text{OH}) \cdot 0.11\text{H}_2\text{O}$, Co_2P and Ni_2P .

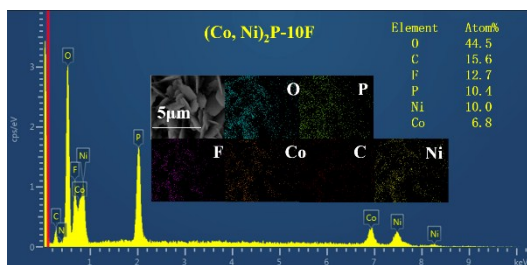
(a)



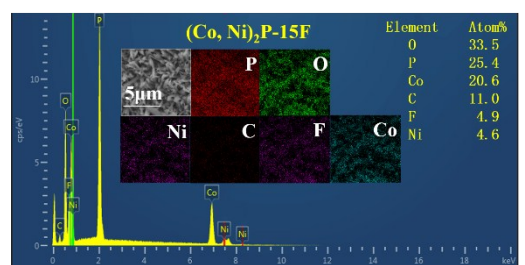
(b)



(c)



(d)



(e)

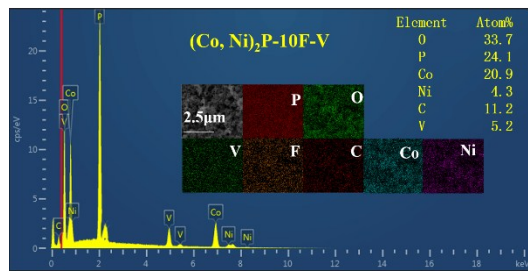


Figure S2 EDS and elemental mappings (inset) of (Co, Ni)₂P (**a**), (Co, Ni)₂P-5F (**b**), (Co, Ni)₂P-10F (**c**), (Co, Ni)₂P-15F (**d**) and (Co, Ni)₂P-10F-V (**e**).

Table S2 The atomic percentages (at. %) for all the metal phosphides

Sample	(Co, Ni) ₂ P	(Co, Ni) ₂ P -5F	(Co, Ni) ₂ P -10F	(Co, Ni) ₂ P -15F	(Co, Ni) ₂ P -10F-V
O	57.2	52.9	44.5	33.5	33.7
Co	8.9	12.6	6.8	20.6	20.9
Ni	8.5	5.8	10.0	4.6	4.3
C	6.1	12.3	15.6	11.0	11.2
N	2.1	/	/	/	/
P	17.2	16.4	10.4	25.4	24.1
F	/	/	12.7	4.9	/
V	/	/	/	/	5.2

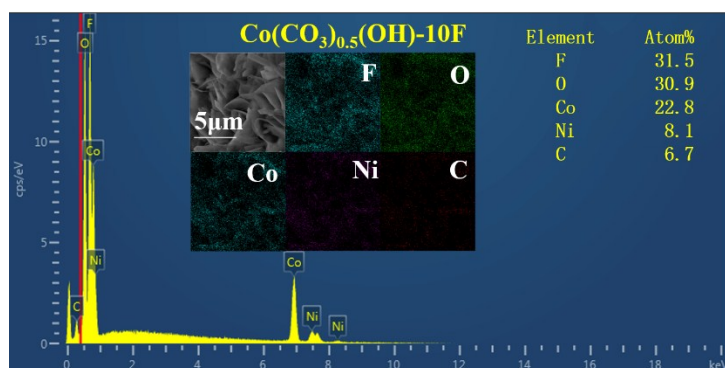


Figure S3 EDS and elemental mappings (inset) of Co(CO₃)_{0.5}(OH)-10F.

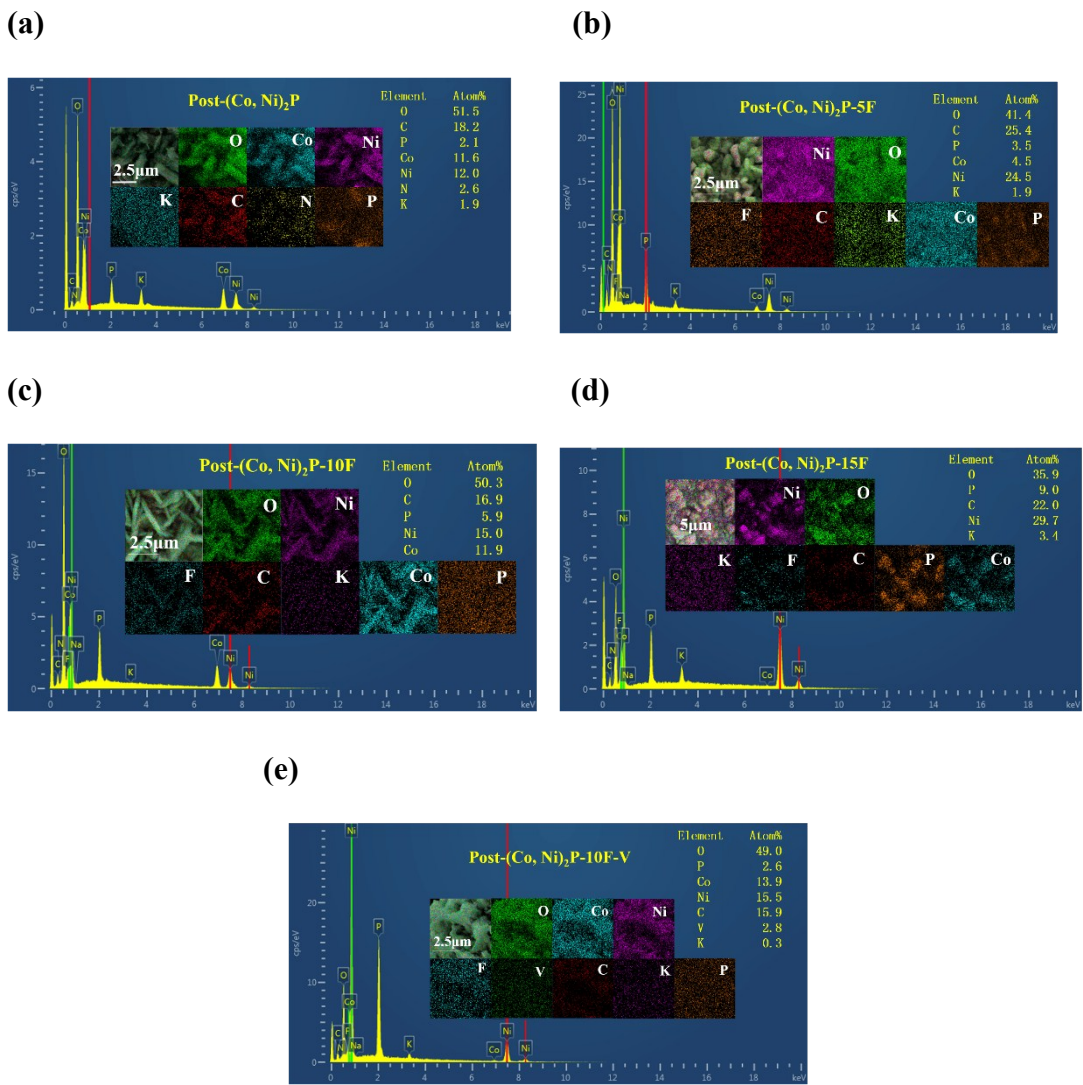


Figure S4 EDS and elemental mappings (inset) of Post-(Co, Ni)₂P (**a**), Post-(Co, Ni)₂P-5F (**b**), Post-(Co, Ni)₂P-10F (**c**), Post-(Co, Ni)₂P-15F (**d**) and Post-(Co, Ni)₂P-10F-V (**e**).

Table S3 The atomic percentages (at. %) for the Post-electrolyzed metal phosphides

Sample	Post-(Co, Ni) ₂ P	Post-(Co, Ni) ₂ P-5F	Post-(Co, Ni) ₂ P-10F	Post-(Co, Ni) ₂ P-15F	Post-(Co, Ni) ₂ P-10F-V
O	51.5	41.4	50.3	35.9	49.0

Co	11.6	4.5	11.9	/	13.9
Ni	12.0	24.5	15.0	29.7	15.5
C	18.2	25.4	16.9	22.0	15.9
N	2.6	/	/	/	/
P	2.1	3.5	5.9	9.0	2.6
F	/	/	/	/	/
V	/	/	/	/	2.8
K	1.9	1.9	/	3.4	0.3

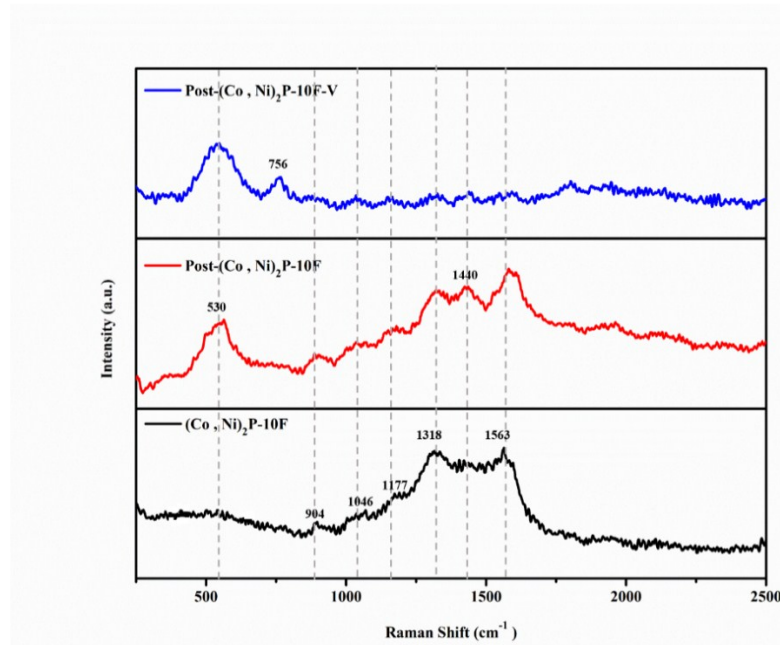


Figure S5 Raman spectra of $(\text{Co}, \text{Ni})_2\text{P}-10\text{F}$, Post- $(\text{Co}, \text{Ni})_2\text{P}-10\text{F}$ and Post- $(\text{Co}, \text{Ni})_2\text{P}-10\text{F-V}$.

(a)

(b)

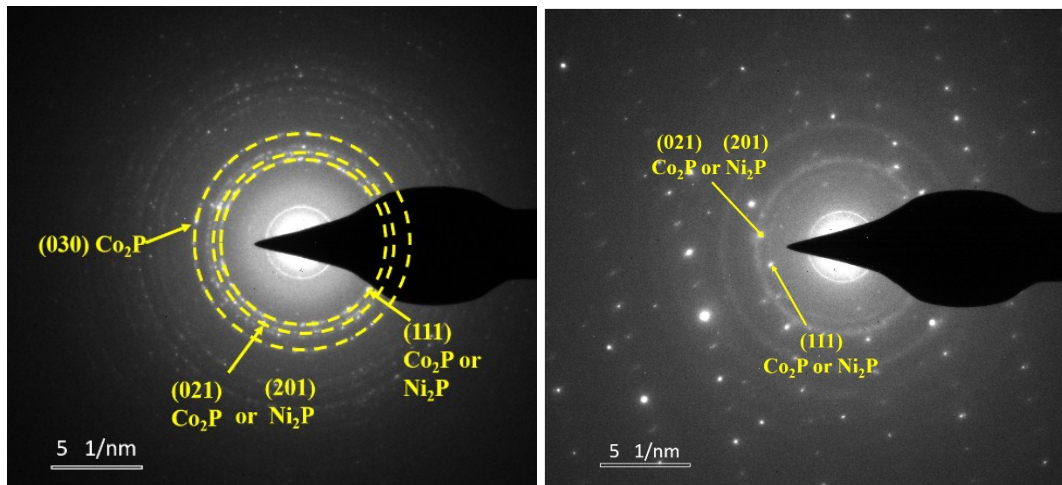


Figure S6 SAED patterns of (Co, Ni)₂P-10F **(a)** and Post-(Co, Ni)₂P-10F **(b)**.

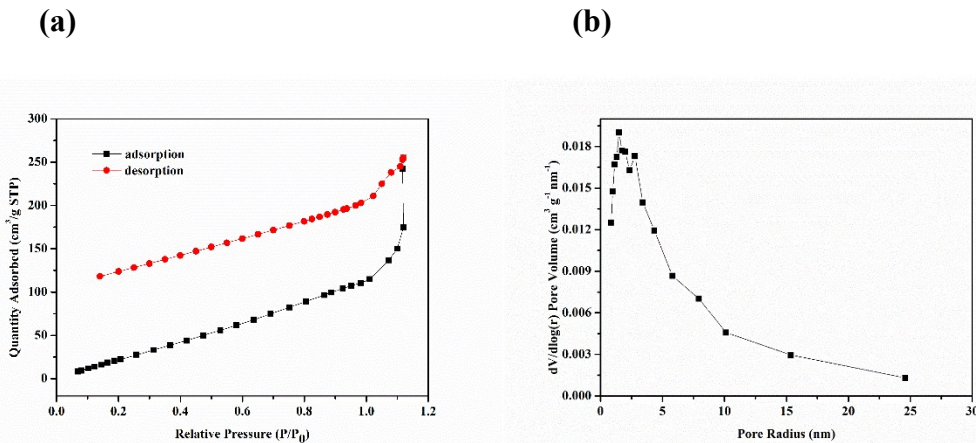


Figure S7 Nitrogen adsorption-desorption isotherms **(a)** and the corresponding pore-size distribution curve of Post-(Co, Ni)₂P-10F **(b)**.

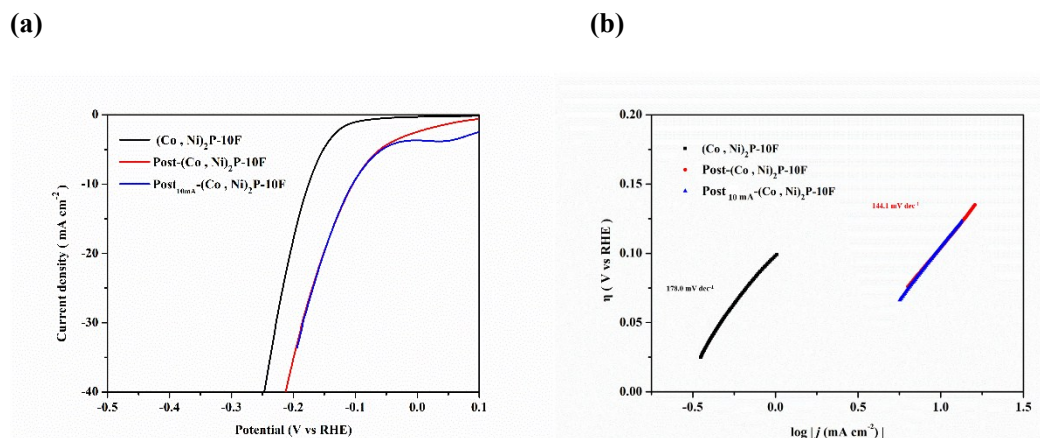


Figure S8 LSV **(a)** and Tafel curves **(b)** of (Co, Ni)₂P-10F, Post-(Co, Ni)₂P-10F and

Post_{10mA}-(Co, Ni)₂P-10F.

Table S4 A comparison of the HER activities for the electrocatalysts

	η_{10} (mV)	Tafel slope (mV dec ⁻¹)	R _{ct} (Ω)	C _{dl} (mF cm ⁻²)	ECSA (cm ²)
(Co, Ni) ₂ P-10F	158	178.0	/	/	/
Post-(Co, Ni) ₂ P	212	109.7	50	8.0	200
Post-(Co, Ni) ₂ P-5F	182	131.3	24.5	11.6	290
Post-(Co, Ni) ₂ P-10F	85	144.1	2.25	14.6	365
Post-(Co, Ni) ₂ P-15F	176	132.8	18.5	12.1	303
Post-(Co, Ni) ₂ P-10F-V	89	140.5	3.5	13.7	343
Pt/C	56	66.6	0.8	44.9	1123

Calculation methods for electrochemical active surface area (ECSA)^{1, 2}

The active surface area of each catalyst was estimated from their electrochemical capacitances, which can be measured using a simple cyclic voltammetry method. We measured the currents in a narrow potential window that no faradic processes were observed, thus the currents should be mostly, if not only, due to the charging of the double layer, which is expected to be linearly proportional to the active surface area. By plotting the capacitive currents ($\Delta J = J_{\text{anode}} - J_{\text{cathode}}$) against the scan rate and following with a linear fit, the double layer capacitance (C) can be estimated as half of the slope. The C can be further converted into ECSA using the specific capacitance. And the specific capacitance for a flat surface is normally between 0.02- 0.06 mF cm⁻². 0.04 mF cm⁻² was used in the following calculations of the ECSA and turnover frequency (TOF) as literatures generally did.

$$\text{ECSA (cm}^{-2}\text{)} = \text{C /0.04}$$

The calculated ECSA was used for the turnover frequency calculations in the following section.

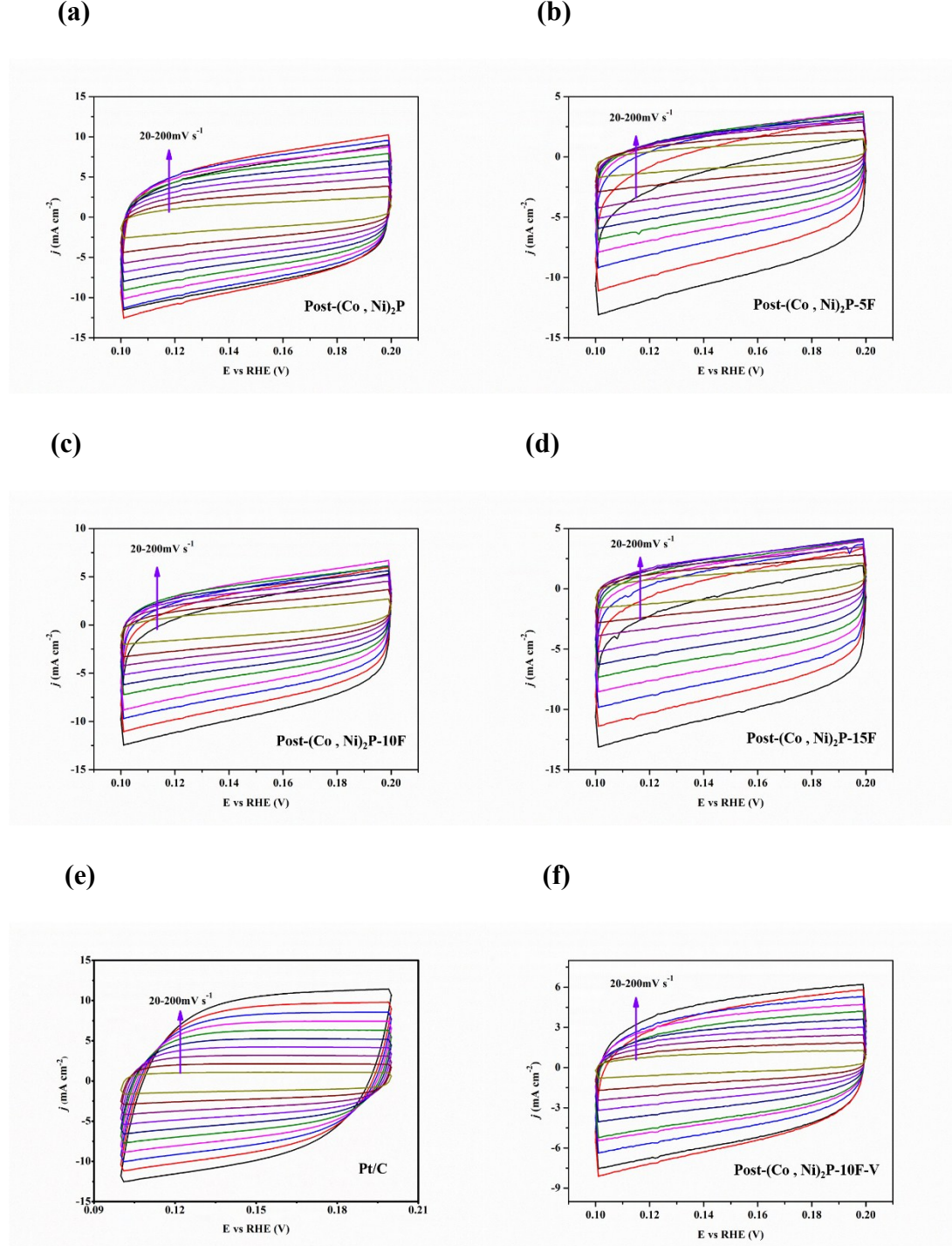


Figure S9 CV curves measured at different scan rates from 20 to 200 mV s⁻¹ in 1 M KOH and capacitive currents at 0.15 V vs RHE as a function of scan rates for

different catalysts: Post-(Co, Ni)₂P (**a**), Post-(Co, Ni)₂P-5F (**b**), Post-(Co, Ni)₂P-10F (**c**), Post-(Co, Ni)₂P-15F (**d**), Pt/C (**e**) and Post-(Co, Ni)₂P-10F-V (**f**).

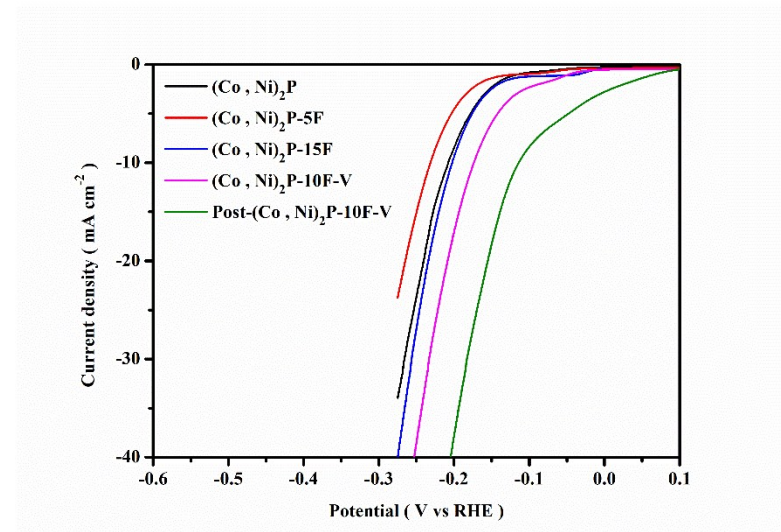


Figure S10 LSV curves at 2 mV s⁻¹ for (Co, Ni)₂P, (Co, Ni)₂P-5F, (Co, Ni)₂P-15F, (Co, Ni)₂P-10F-V and Post-(Co, Ni)₂P-10F-V.

Table S5 Comparison of the HER activities of (Co, Ni)₂P-10F with other catalysts

Electrocatalyst	Electrolyte	η_{10} (mV)	Tafel slope (mV dec ⁻¹)	Ref.
CoP/CC	1 M KOH	209	129	³
Fe-Co ₂ P/NCNTs	0.5M H ₂ SO ₄	104	58	⁴
Co ₂ P	0.5 M H ₂ SO ₄	134	71	⁵
CoP NS/CC	1 M KOH	90	68	⁶
CoP@NF	1 M KOH	86.6	70.9	⁷
CoNiP@NF	1 M KOH	155	134	⁸
Fe ₂ P@rGO	0.5 M H ₂ SO ₄	101	55.2	⁹
3D-NiCoP	1 M KOH	105	79	¹⁰

Petaloid FeP/C	1 M KOH	185	93	11
CoP/CFP-H	0.5 M H ₂ SO ₄	128.1	49.7	12
MoP-RGO	1 M KOH	152	74	13
WP@PC	0.5 M H ₂ SO ₄	173	59.3	14
Post-(Co, Ni)₂P-10F	1 M KOH	85	144.1	This work

Table S6 A comparison of HER overpotentials (η_{10}) for the electrocatalysts before and after electrolysis at -0.1 V vs RHE

Before electrolysis	η_{10} (mV)	After elelctrolysis	η_{10} (mV)
(Co, Ni) ₂ P	188	Post-(Co, Ni) ₂ P	212
(Co, Ni) ₂ P-5F	212	Post-(Co, Ni) ₂ P-5F	182
(Co, Ni) ₂ P-10F	158	Post-(Co, Ni) ₂ P-10F	85
(Co, Ni) ₂ P-15F	184	Post-(Co, Ni) ₂ P-15F	176
(Co, Ni) ₂ P-10F-V	155	Post-(Co, Ni) ₂ P-10F-V	89

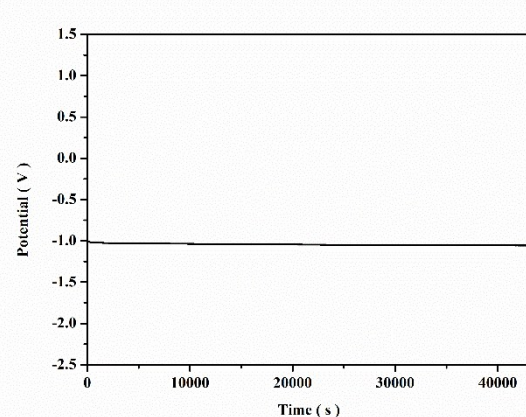


Figure S11 Chronopotentiometry data (V - t) recorded for Post-(Co, Ni)₂P-10F at HER current density of -10 mA cm⁻².

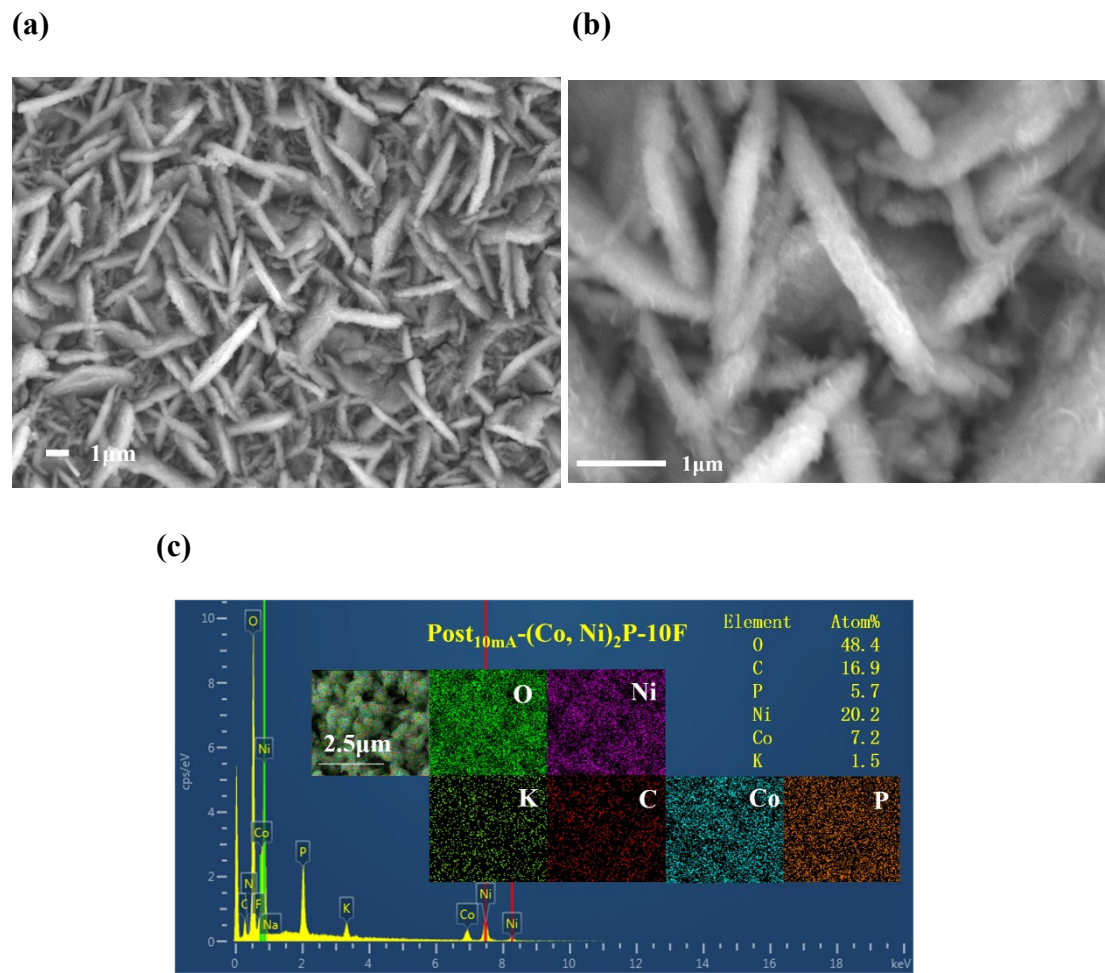
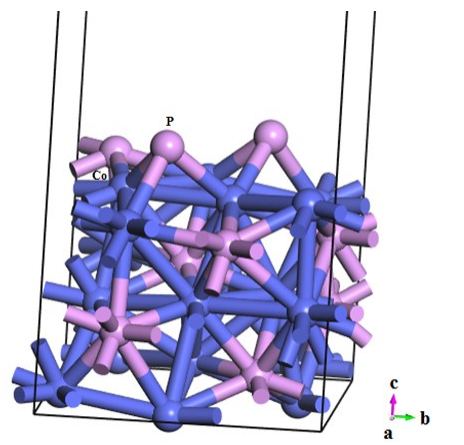
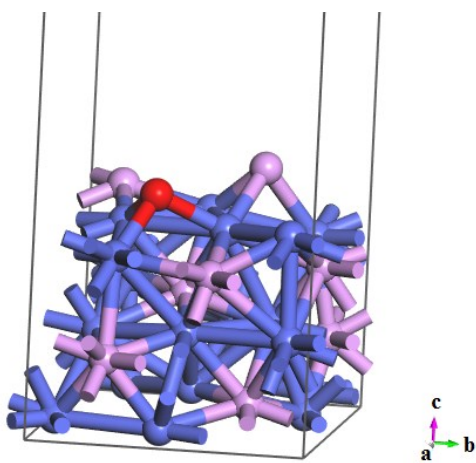


Figure S12 SEM images (a, b), EDS and elemental mappings (inset) of $\text{Post}_{10\text{mA}}\text{-(Co, Ni)}_2\text{P-10F}$ (c).

(a)



(b)



(c)

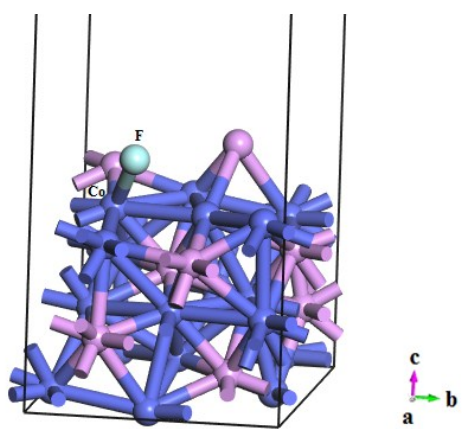
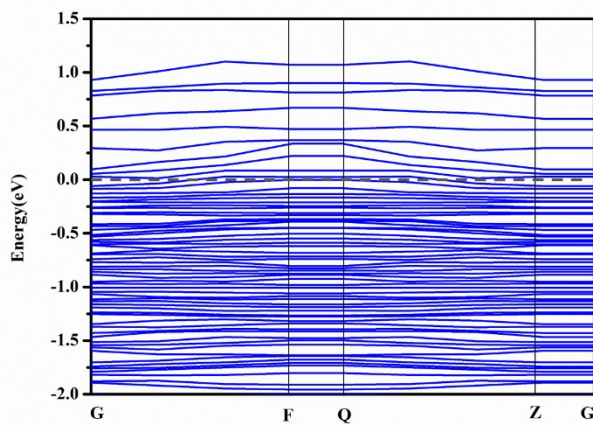
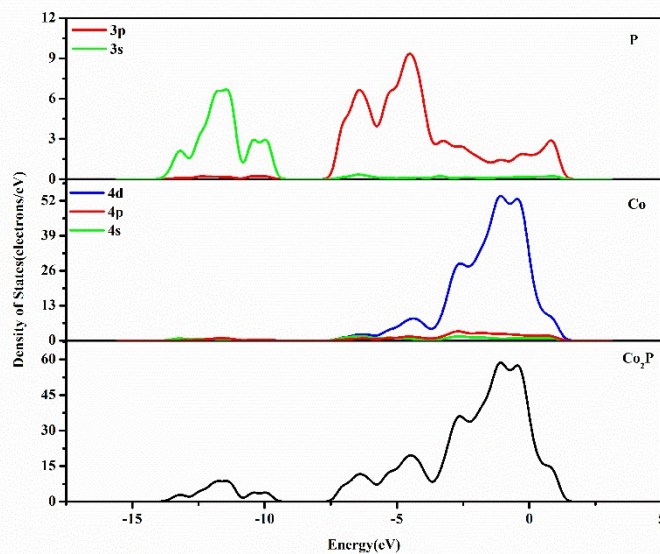


Figure S13 Crystal structures of Co_2P (a), O-partially substituted Co_2P (b) and F-partially substituted Co_2P (c). Color codes: pink, P; blue, Co; red, O; sapphire, F.

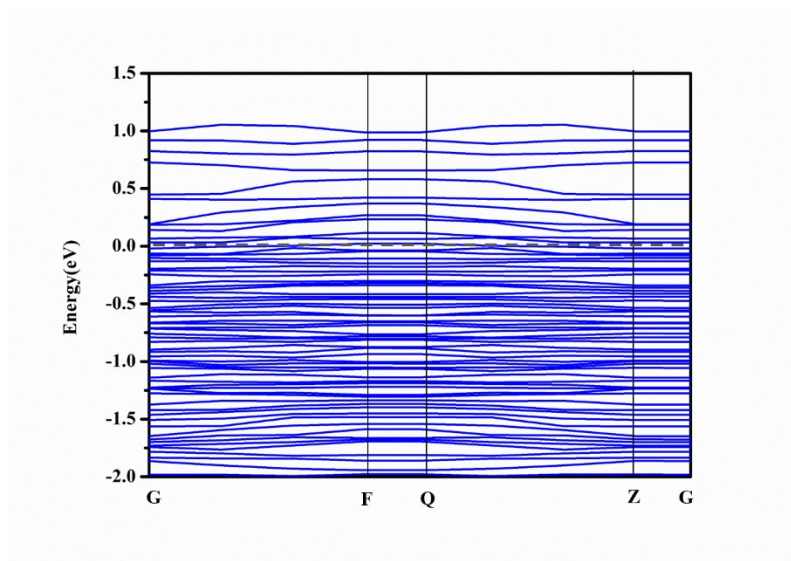
(a)



(b)



(c)



(d)

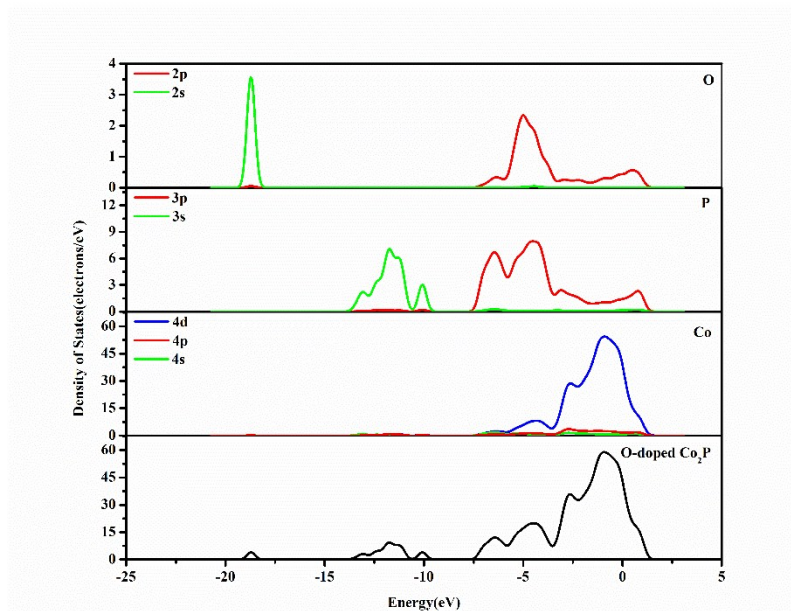


Figure S14 Band structures (**a, c**), the calculated total DOS (black) and partial DOS (**b, d**) of Co₂P (**a, b**) and O-doped Co₂P (**c, d**). In the PDOS, blue, red and green lines represent d, p and s orbitals, respectively. The Fermi level is set to zero.

References:

- 1 Y. Y. Chen, Y. Zhang, W. J. Jiang, X. Zhang, Z. Dai, L. J. Wan and J.S. Hu, *ACS Nano* 2016, **10**, 8851-8860.
- 2 S. T. Finn and J. E. Macdonald, *ACS Appl. Mater. Interfaces* 2016, **8**, 25185-25192.
- 3 J. Tian, Q. Liu, A. M. Asiri and X. Sun, *J. Am. Chem. Soc.* 2014, **136**, 7587-7590.
- 4 Y. Pan, Y. Liu, Y. Lin and C. Liu, *ACS Appl. Mater. Interfaces* 2016, **8**, 13890-13901.

- 5 Z. Huang, Z. Chen, Z. Chen, C. Lv, M. G. Humphrey and C. Zhang, *Nano Energy* 2014, **9**, 373-382.
- 6 X.Y. Yan, S. Devaramani, J. Chen, D. L. Shan, D. D. Qin, Q. Ma and X.Q. Lu, *New J. Chem.* 2017, **41**, 2436-2442.
- 7 P. Guo, Y.X. Wu, W.M. Lau, H. Liu and L.M. Liu, *Int. J. Hydrogen Energ.* 2017, **42**, 26995-27003.
- 8 A. Han, H. Chen, H. Zhang, Z. Sun and P. Du, *J. Mater. Chem. A* 2016, **4**, 10195-10202.
- 9 M. Liu, L. Yang, T. Liu, Y. Tang, S. Luo, C. Liu and Y. Zeng, *J. Mater. Chem. A* 2017, **5**, 8608-8615.
- 10 B. Ma, Z. Yang, Y. Chen and Z. Yuan, *Nano Res.* 2019, **12**, 375-380.
- 11 F. Wang, X. Yang, B. Dong, X. Yu, H. Xue and L. Feng, *Electrochim. Commun.* 2018, **92**, 33-38.
- 12 S. H. Yu and D. H. C. Chua, *ACS Appl. Mater. Interfaces* 2018, **10**, 14777-14785.
- 13 Z. Wu, M. Song, Z. Zhang, J. Wang and X. Liu, *J. Colloid. Interf. Sci.* 2019, **536**, 638-645.
- 14 J. S. Li, S. Zhang, J. Q. Sha, H. Wang, M. Z. Liu, L. X. Kong and G. D. Liu, *ACS Appl. Mater. Interfaces* 2018, **10**, 17140-17146.